

# Micrometer size polarisation independent depletion-type photonic modulator in Silicon On Insulator

F. Y. Gardes, K. L. Tsakmakidis, D. Thomson, G. T. Reed, G. Z. Mashanovich, and O. Hess

University of Surrey, Advanced Technology Institute, Daphne Jackson Building, Guildford, GU2 7XH, UK

[F.Gardes@surrey.ac.uk](mailto:F.Gardes@surrey.ac.uk)

D. Avitabile

University of Surrey, Department of Mathematics

**Abstract:** The trend in silicon photonics, in the last few years has been to reduce waveguide size to obtain maximum gain in the real estate of devices as well as to increase the performance of active devices. Using different methods for the modulation, optical modulators in silicon have seen their bandwidth increased to reach multi GHz frequencies. In order to simplify fabrication, one requirement for a waveguide, as well as for a modulator, is to retain polarisation independence in any state of operation and to be as small as possible. In this paper we provide a way to obtain polarisation independence and improve the efficiency of an optical modulator using a V-shaped pn junction base on the natural etch angle of silicon, 54.7 deg. This modulator is compared to a flat junction depletion type modulator of the same size and doping concentration.

© 2007 Optical Society of America

**OCIS codes:** (060.4080) Modulation ; (250.7360) waveguide modulators; (250.5300) Photonic integrated circuits

---

## References and links

1. L. Liao, D. Samara-Rubio, M. Morse, A. Liu, D. Hodge, D. Rubin, U. D. Keil and T. Franck, High speed silicon mach-zehnder modulator, *Opt. Express* 13, 3129-3135 (2005).
2. A. Liu, R. Jones, O. Cohen, D. Hak, R. Nicolaescu, A. Fang, and M. Paniccia, "An all-silicon Raman laser," *Nature* 433, 292-294 (2005).
3. Y.-H. Kuo, Y. K. Lee, Y. Ge, S. Ren, J. E. Roth, T. I. Kamins, D. A. B. Miller, and J. S. Harris, "Strong quantum-confined Stark effect in germanium quantum-well structures on silicon," *Nature* 437, 1334-1336 (2005).
4. J. Wei, G. Lanlan, C. Xiaonan, and R. T. Chen, "80-micron interaction length silicon photonic crystal waveguide modulator," *Appl. Phys. Lett.* 87, 221105-1 (2005).
5. F. Y. Gardes, G. T. Reed, N. G. Emerson, and C. E. Png, "A sub-micron depletion-type photonic modulator in silicon on insulator," *Opt. Express* 13, 8845-8854 (2005).
6. G. Z. Masanovic, V. M. N. Passaro, and G. T. Reed, "Coupling to nanophotonic waveguides using a dual grating-assisted directional coupler," *IEE Proceedings: Optoelectronics* 152, 41-48 (2005).
7. W. R. Headley, G. T. Reed, S. Howe, A. Liu, and M. Paniccia, "Polarization-independent optical racetrack resonators using rib waveguides on silicon-on-insulator," *Appl. Phys. Lett.* 85, 5523-5 (2004).
8. R. A. Soref and B. R. Bennett, "Kramers-Kronig analysis of electro-optical switching in silicon," presented at Proc. SPIE: Integrated Optical Circuit Engineering IV, 16-17 Sept. 1986, Cambridge, MA, USA, 1987, 32-37.
9. Silvaco International, 4701 Patrick Henry Drive, Bldg 1, Santa Clara, CA 94054, <http://www.silvaco.com>.
10. K. L. Tsakmakidis, C. Hermann, A. Klaedtke, C. Jamois, and O. Hess, "Systematic modal analysis of 3-D dielectric waveguides using conventional and high-accuracy nonstandard FDTD algorithms," *IEEE Photon. Technol. Lett.* 17, 2598-2600 (2005).

## 1. Introduction

Silicon photonics has experienced rapid development in recent years and several significant results have been reported, demonstrating the viability of the technology [1][2][3][4][5]. In the design of an optical modulator, four factors are of major importance, the waveguide size, the bandwidth, the efficiency ( $L\pi.V\pi$ ) and polarisation independence. The use of depletion modulators using a pn junction is an answer to the bandwidth requirement in silicon photonics as the speed is not limited by the minority carrier lifetime. The drawback of such a technology is that the length required to achieve a  $\pi$  phase shift in a rib waveguide is in the order of millimeters [5]. In order to improve the real estate of depletion modulators on an optical chip, the efficiency of these devices need to be improved. The solution could be to use smaller waveguide size as proposed in Ref. [5], where the confinement of the mode in a submicron waveguide increase the efficiency of the modulator. The issue with submicron waveguides is the need for efficient optical coupling for TE and TM polarization [6], as well as losses in the waveguide due to surface roughness and fabrication tolerances. In this paper, we try to provide a solution to the remaining issues, by inserting a pn junction in a micrometer size waveguide which was demonstrated to be polarization independent in Ref. [7]. The proposed modulator is a pn junction formed by a V-shape structure, as shown in Fig. 1(b). This structure will be compared to a more common structure [5] where a flat pn junction is used as shown in Fig. 1(a).

## 2. Device modelling

### 2.1. Optical modelling

The optimal design of the proposed optical modulator relies critically, inter alia, on the high-accuracy modelling of the dielectric waveguide structure. The high-index contrast between the silicon and silicon-oxide regions results in a pronounced localization of the weak quasi-TE and quasi-TM field-components at the corners of the dielectric heterostructure, where occasionally they can become comparable in magnitude with the strong field-components. This, combined with the non-piecewise-linear variation of the refractive indices at the middle region, invalidates the use of approximate semi-analytic techniques, such as the effective index method, and at the same time it may render an accurate deployment of commercial mode-analysis tools overly difficult. To overcome such limitations, and to reliably characterize the birefringence-free, single-mode waveguide, we developed a fully-vectorial finite-difference frequency-domain (FV-FDFD) mode-solving method, whose accuracy and lattice convergence have been thoroughly tested in our previous works [10][11]. The method computes the E- or H-field eigenvectors of the vectorial wave equation and takes into account the polarization, vector properties and discontinuity of the guided modes at the dielectric interfaces, including the corner regions. The active modulators are introduced to the model, by fitting the change in refractive index provided by the simulation of the carrier distribution in the devices into the mode solver. The effective index change of the waveguides for different voltages is then determined, hence calculating the optimum length in order to achieve a  $\pi$  phase shift (Eq. (1) below). The same method has been used to characterise the transient behaviour. The carrier concentration changes at any given bias, are introduced into the mode solver for different transient times, hence giving a dynamic change in effective index. Thus using Eq. (1) below, the phase shift induced with time can be evaluated.

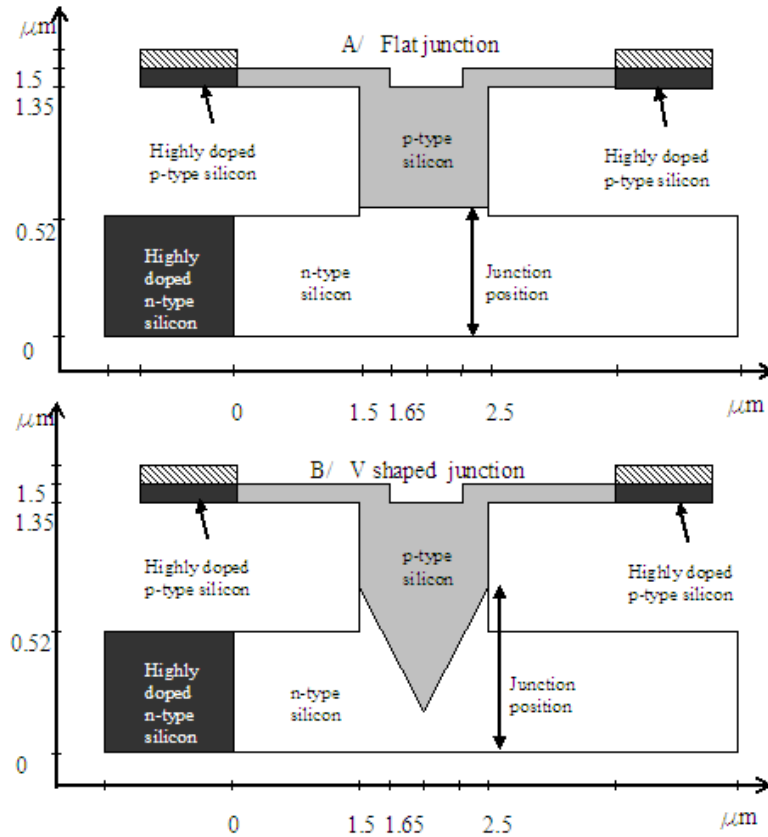


Fig. 1. (A). Flat pn junction optical modulator in silicon on insulator. (B). V-shape pn junction optical modulator in silicon on insulator.

Temperature	300 K
Wavelength	1.55 $\mu\text{m}$
Si refractive index	3.47
SiO <sub>2</sub> refractive index	1.44

Table 1. Optical simulation parameters.

## 2.2. Electrical modelling

The devices were modeled for both their static and dynamic behavior using Atlas, the device simulation package from Silvaco [9]. Atlas device simulation framework predicts the electrical behavior of semiconductor devices. It provides a physics-based platform to analyse DC and time domain responses for semiconductor based technologies, by solving the equations which describe semiconductor physics such as Poisson's equation and the charge continuity equations for holes and electrons. The simulator has been used to predict the free carrier concentrations in the waveguiding region of the devices for both DC and transient biasing conditions. The change in the free carrier profile is then converted to refractive index profile in the device using the expressions given by Soref and Bennett (Eq. (2) of [8]). To determine the voltage associated with a  $\pi$ -phase shift, the change in concentration of free carriers must be known. Assuming

a non uniform change in refractive index, the active device length required to produce the refractive index change associated with a  $\pi$ -phase shift is obtained approximately from the change in effective index.

$$\Delta n_{\text{eff}} = \frac{\lambda}{2L_{\pi}} \quad (1)$$

Where  $\lambda$  is the operating wavelength,  $L_{\pi}$  is the active length of the modulator and  $\Delta n_{\text{eff}}$  is the change in effective index induced by the change in refractive index  $\Delta n$  in the waveguide. At  $1.55 \mu\text{m}$ , which is also the operating wavelength for all simulations here, the refractive index change  $\Delta n$  is given by

$$\Delta n = \Delta n_e + \Delta n_h = -[8.8 \times 10^{-22} \times \Delta N_e + 8.5 \times 10^{-18} \times \Delta N_h^{0.8}] \quad (2)$$

where  $\Delta n_e$  is the change in refractive index resulting from the change in free electron concentration,  $\Delta n_h$  is the change in refractive index resulting from the change in free hole concentration,  $\Delta N_h$  is the change in free holes concentration and  $\Delta N_e$  is the change in free electron concentration.

Surfaces of the waveguides are passivated with SiO <sub>2</sub>	
Hole carrier lifetime	300 ns
Electron carrier lifetime	700 ns
N-type	$1 \times 10^{18}$ ions/cm <sup>3</sup>
P-type	$1 \times 10^{18}$ ions/cm <sup>3</sup>
N and P - type resistive contact	$(1 \times 10^{19}$ ions/cm <sup>3</sup> )
Si background carrier concentration	$(1 \times 10^{15}$ ions/cm <sup>3</sup> )

Table 2. Electrical simulation parameters.

### 3. Simulation results

#### 3.1. Waveguide structures

The two modulators are based on a polarisation independent, single mode rib waveguide published in Ref. [7]. The dimensions are: Height,  $H=1.35 \mu\text{m}$ , Width,  $W=1 \mu\text{m}$  and etch depth,  $E=0.83 \mu\text{m}$ . The modulator structures are based on a wing design, proposed by Liao et al for the MOS capacitor modulator [1]. Both use the depletion of a pn junction in order to change the effective index of the mode propagating in the waveguide. The main difference between the modulators is the shape of the pn junction. Figure 1(B) shows the proposed polarisation independent V-shaped junction, this is created with an angle of 54.7 degrees which is the natural etch angle of silicon. Figure 1(A) shows a flat pn junction across the waveguide. As the two waveguides are approaching polarisation independence due to their design structure the aim is to show the differences in the phase shift for TE and TM polarisation between both designs while applying a reverse bias.

#### 3.2. Efficiency of the modulator and positioning of the junction inside the waveguide

The simulations undertaken below are to determine the polarisation independence of the waveguide during modulation. Figures 2(A) and 2(B) show the phase shift achieved for different junction positions and voltages. Junction position is measured from the buried oxide in the case of the flat junction. In the case of the V-shaped junction, the position of the intersection between the sidewalls and the top of the 'V' is measured from the buried oxide (see Fig. 1). Figure 2(A)

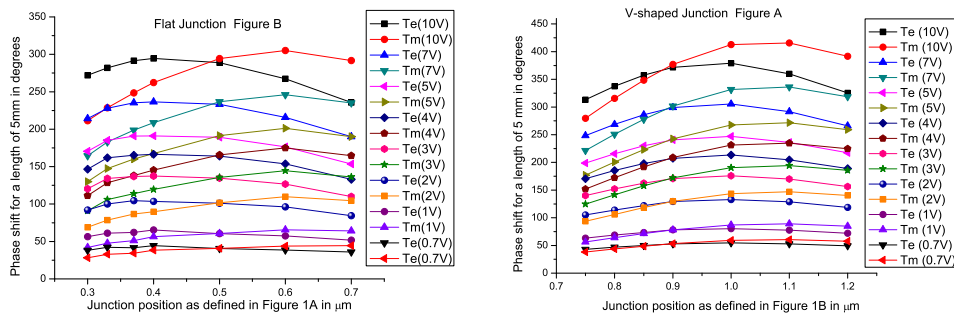


Fig. 2. (A).Phase shift modulation dependence for TE and TM using a flat pn junction. (B). Phase shift modulation dependence for TE and TM using a V-shaped pn junction.

shows similar results for the flat junction and Fig. 2(B) shows the simulation resulting from the V-shape junction. Each curve is a plot of the phase shift achieved, at a given bias voltage, as a function of position of the junction. In order to achieve polarisation independence during modulation the positioning of the junction inside the waveguide was changed and the phase shift was calculated for TE and TM, for reverse bias voltages varying from 0 to 10 volts. Figures 2(A) and 2(B) show that when the TE and TM curves intersect at a given bias voltage, polarisation independence is achieved for a specific junction position for both type of junctions and is consistently observed at the same depth for reverse bias varying between 0 and 10 volts. For the particular rib waveguide studied in this paper, polarisation independence is obtained at a depth of  $0.87 \mu\text{m}$  for the v-shaped junction and  $0.5 \mu\text{m}$  for the flat junction. Furthermore by considering taking the structure where polarisation independence is achieved, the best  $L\pi.V\pi$  efficiency is obtained for the v-shaped junction with  $L\pi.V\pi=2.5 \text{ V.cm}$  compared to  $L\pi.V\pi=3.1 \text{ V.cm}$  for the flat junction.

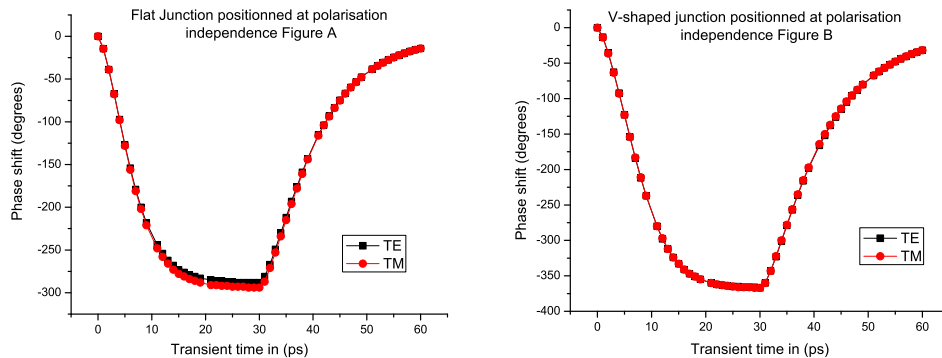


Fig. 3. (A). Phase shift against transient time for TE and TM for the flat junction. (B). Phase shift against transient time for TE and TM for the V-shaped junction.

These results show that the V-shaped pn junction can achieve the same efficiency as the modulator proposed in Ref. [5] without the problems involved with submicron waveguides. The efficiency of a modulator comes from the overlap of the mode profile and the refractive index variation due to the carrier distribution change. Hence the more carriers that are removed

from the overlap region for a specific reverse bias, then the better the efficiency will be. The p type region, also play an important role in the efficiency as the concentration holes plays a more dominant role than the concentration of electrons in the refractive index change. Intuitively one would expect TE and TM modes to be affected equally if a junction could be fabricated at 45 degrees to the major TE and TM axes if the TE and TM axes were identical, but simply rotated by 90 degrees with respect to one another. However, because the mode shapes are different, some other angle is likely to be optimal. However, the flat junction will definitely not be optimal and will probably shows the most extreme polarisation dependence. That can be mitigated to some extent, by translation of the junction vertically. Thus it is not surprising that the flat junction shows more polarisation dependence than the V-shaped junction, which in turn, must be nearer to the optimal angle than the flat junction. The V-shaped junction will also be more phase efficient than the flat junction, simply because the V-shape results in a greater net length of the junction and hence in more net depletion.

The next step is to determine the intrinsic bandwidth of both modulators. This is done by calculating the phase shift against transient time and is shown in Figs. 3(A) and 3(B) for TE and TM polarisation and for the flat and V junction, respectively.

The transients show that the rise and fall time are similar for the both types of junctions. For this type of doping, the V-shape junction has a rise time of 13 ps and a fall time of 23 ps for both TE and TM. For the flat junction the rise time is 12ps and the fall time is 21ps for both TE and TM. In both cases, this corresponds to an intrinsic bandwidth in excess of 15 GHz.

#### 4. Conclusion

We have studied two 5 mm long depletion type modulators inserted in a micrometer size rib waveguide, that has already been demonstrated in Ref. [7] to be polarisation independent and single mode. The two modulators have been simulated to maintain polarisation independence for a specific position of the junction inside the waveguide during modulation. The intrinsic bandwidth has been calculated to be above 15 GHz for both modulators while retaining polarisation independence. Furthermore the  $L\pi.V\pi$  performance metric for the V-shaped modulator equals that of the modulator proposed in Ref. [5] for the submicron depletion modulator, and exceeds that of [1]. The proposed modulator is therefore a serious candidate for optical modulation in silicon photonics easing some of the difficulties arising from designs based around sub-micrometer waveguides, whilst retaining polarisation independence and an efficiency comparable to sub-micrometer waveguide based depletion modulators.